Cellular and Molecular Bioengineering, Vol. 8, No. 4, December 2015 *(© 2015)* pp. 577–590
DOI: 10.1007/s12195-015-0403-x

The Influence of Adipose-Derived Stem Cells Induced into Endothelial Cells on Ectopic Vasculogenesis and Osteogenesis

Jelena G. Najdanović,[1] Vladimir J. Cvetković,[2] Sanja Stojanović,[1] Marija Đ. Vukelić-Nikolić,[1] Milica N. Stanisavljević,[3] Jelena M. Živković,[1] and Stevo J. Najman[1]

[1]Institute of Biology and Human Genetics; Department for Cell and Tissue Engineering, Faculty of Medicine, University of Niš, 18000 Niš, Serbia; [2]Department of Biology and Ecology, Faculty of Science and Mathematics, University of Niš, 18000 Niš, Serbia; and [3]Scientific Research Center for Biomedicine, Faculty of Medicine, University of Niš, 18000 Niš, Serbia

(Received 8 March 2015; accepted 17 June 2015; published online 30 June 2015)

Associate Editor Alyssa Panitch oversaw the review of this article.

Abstract—Established vascular network has a crucial importance in bone regeneration. Adipose-derived stem cells (ADSCs) can be differentiated *in vitro* towards endothelial cells (ECs) that give a possibility for their application in bone tissue engineering (BTE). The aim of our study was to examine the influence of ADSCs *in vitro* induced into ECs on vascularization and osteogenic process in subcutaneous implants. Induced ADSCs were implanted subcutaneously into BALB/c mice, in combination with the bone mineral matrix carrier (BC) and platelet-rich plasma (PRP), parallel with the implants without the cells. The combination of BC, PRP and ADSCs induced into ECs increased vascularization in subcutaneous implants that was shown through endothelial-related gene expression, high percentage of vascularization and VEGFR-2 immunoexpression. Osteocalcin immunoexpression, relative expression of osteopontin gene, and histological analysis showed that osteogenic process was more pronounced when the carrier was loaded with ADSCs induced into ECs which was associated with strong vascularization in cellularized implants. In implants without the cells vasculogenesis was initially stimulated, but vascular network was unsustainable at later observation points. Therefore, the approach that includes ADSCs *in vitro* induced into ECs combined with BC and PRP can be a good strategy for improving vascularization in bone regeneration and BTE.

Keywords—Endothelial induction, Vascularization, Platelet-rich plasma, Bone mineral matrix, Bone tissue engineering.

ABBREVIATIONS

BTE	Bone tissue engineering
ADSCs	Adipose-derived stem cells
ECs	Endothelial cells
BC	Bone mineral matrix carrier
PRP	Platelet-rich plasma
SVF	Stromal vascular fraction
DMEM	Dulbecco's Modified Eagles Minimal Essential Medium
P03	Third passage
ECP	The implants consisted of ADSCs *in vitro* induced into ECs, BC and PRP
CP	The implants consisted of BC and PRP
OC	Osteocalcin

INTRODUCTION

Bone tissue is highly vascularized tissue, made up from bone matrix, functionally and spatially interconnected bone cells and blood vessels.[24] Vascular network removes metabolites from bone tissue, thus providing constant oxygen and essential nutrients supply.[69] Therefore, establishing of vascular network is crucial for successful bone tissue regeneration.[24]

Vascular network formation occurs through the processes of vasculogenesis and angiogenesis. Vasculogenesis is the process of forming new blood vessels from mesodermal precursors in the embryo, while angiogenesis represents the formation of new blood vessels from the existing differentiated endothelial cells, which proliferate and migrate.[28,68] Considering the fact

Address correspondence to Jelena G. Najdanović, Institute of Biology and Human Genetics; Department for Cell and Tissue Engineering, Faculty of Medicine, University of Niš, 18000 Niš, Serbia. Electronic mail: jella82@gmail.com, biovlada@yahoo.com, s.sanja88@gmail.com, marijavukelic@yahoo.com, stanisavljevic.milica@yahoo.com, jelena.zivkovicmf@yahoo.com, stevo.najman@gmail.com

that vascular network needs to be established before the formation of bone tissue, vasculogenesis and angiogenesis have obtained great attention in the field of bone tissue engineering (BTE).

Diffusion of oxygen limited to around 150 μm from capillary in the active tissue is the main problem in large tissue-engineered constructs.[55,69] When vascularization is delayed after the tissue damage, one of the consequences is the development of necrotic cores.[41]

To date, the problem of inadequate vascularization in BTE was accessed through various approaches including the modification of architecture and interconnection of pores of the biomaterial carrier,[10] addition of one,[4,61] or multiple pro-angiogenic growth factors into the implants which can stimulate the formation of blood-vessels at different stages of vascular network formation.[44,56] Co-culturing systems,[63,69] mechanical stimulation,[6,62] pre-vascularization of tissues or implants with intact microvessels or cultured vascular cells,[59] implantation into the highly vascularized areas or pre-seeding the implants with cells which secret chemoattractants for recruiting host cells and microvessels[53] were also applied in order to improve vascularization in BTE.

The novel strategies in BTE involve interactions between the scaffolds, cells and biological signaling molecules. Those interactions can be accomplished by mimicking the native tissues which are composed of so-called "biological triad"—the cells, signaling mechanisms between them and extracellular matrix (ECM).[43] To provide a background in which the "biological triad" principle can be accomplished, we bioengineered the implants by combining adipose-derived stem cells (ADSCs), bone mineral matrix carrier (BC), and platelet-rich plasma (PRP). ADSCs induced into ECs were used as a vasculogenic component, while PRP and BC were applied in order to ensure osteogenic milleu in implants.

White adipose tissue is an attractive source of mesenchymal cells, due to relatively easy isolation procedure,[8,37] its accessibility and great yield of cells with the potential of differentiating into various cell lines.[15,32] ADSCs were our choice because of their potential to differentiate into endothelial cells (ECs), and form vascular-like network *in vitro*.[34] ADSCs can be implanted, orthotopic or ectopic, loaded on a bone substitute biomaterial which can serve as a cell carrier. Commercial bovine bone mineral matrix Bio-Oss® (Geistlich-Pharma, Wolhusen, Switzerland) is highly biocompatible and osteoconductive thus fulfilling the requirements for the role of ADSCs carrier.[45] Generally, hydroxyapatite (HAp)-based biomaterials are excellent carriers of osteoinductive growth factors.[3] Platelet-rich plasma (PRP) can serve as an initial source of growth factors[1] because the events at the cellular level, that occurs after the tissue damage, are notably controlled by growth factors released from the platelets.[70] Another benefit of applying PRP combined with BC and cells is the ability of PRP to form fibrin mesh which acts as a tissue glue, thus preventing displacement of the biomaterial after implantation[33] and enabling cell adhesion, migration and proliferation after the activation of PRP.[64]

The aim of our study was to examine the effect of ADSCs isolated from mice epididymal adipose tissue and *in vitro* induced into ECs on vascularization and osteogenic process in mice subcutaneous implants. According to our knowledge, our study is the first one where ADSCs, *in vitro* induced into ECs, were applied onto biomaterial carrier (BC) formed of bone mineral matrix, combined with platelet-rich plasma (PRP), and implanted into an ectopic site. We have hypothesized that implants constructed in this manner will elicit vasculogenesis which is precondition for osteogenic process.

MATERIALS AND METHODS

Isolation and Endothelial Differentiation of ADSCs

ADSCs were obtained from epididymal mice adipose tissue in accordance with previously described methods with minor modifications.[16,57] Isolated tissue was digested using Collagenase type I (Sigma-Aldrich, Germany) dissolved in standard cell culture media DMEM (Dulbecco's Modified Eagles Minimal Essential Medium, PAA Laboratories GmbH, Austria) at the concentration of 2000 I.U. per 1 mL. Digestion was performed in a water bath for 45 min, at 37 °C, with agitation. To remove the tissue debris, digested tissue was filtered through a 180 μm mesh. The tubes with digested tissue were centrifuged at 4 °C for 10 min, at 1500 rpm. White, "lipid" ring from the top of the tubes and supernatant were removed, and pellet containing stromal vascular fraction (SVF) was resuspended. Viable cells were counted using Trypan blue dye exclusion method, seeded at density of 1×10^6 per 25 cm^2 growth area, and cultivated in DMEM supplemented with 10% foetal calf serum (FCS, PAA Laboratories GmbH, Austria), 1% antibiotic–antimycotic solution (PAA Laboratories GmbH, Austria), and 2 mM L-glutamine (PAA Laboratories GmbH, Austria). The changes in cell morphology were monitored on inverted light microscope (Observer Z1, Carl Zeiss, Germany), under phase-contrast. The images were acquired using the camera AxioCam HR (Carl Zeiss, Germany) and the software Zeiss Axiovision (Carl Zeiss, Germany).

Endothelial Differentiation

After the third passage (P03), the cells were counted by using Trypan blue dye exclusion method and seeded

into 24-well cell culture plates at density 0.5×10^4/well. Two types of cell cultures were cultivated in the plates-ADSCs differentiated towards ECs by using EndoPrime Kit (PAA Laboratories GmbH, Austria) for endothelial differentiation, and ADSCs cultivated in DMEM without the addition of endothelial factors. The kit consists of cell culture media with L-glutamine and the mixture of Vascular endothelial growth factor (VEGF), Epidermal growth factor (EGF), Insulin-like growth factor (IGF), Fibroblast growth factor (FGF), hydrocortisone, heparin and ascorbic acid. The media was also supplemented with 5% FCS and 1% antibiotic–antimycotic solution.

Immunocytochemistry

Stem cell phenotype was assessed 1 day after P03, using positive (anti-CD29, 1:400, ab52971, Abcam, USA), and negative (anti-CD14, 1:1000, ab106285, Abcam, USA) stem cell markers. Antibody to vascular endothelial growth factor receptor 2 (anti-VEGFR-2, 1:100, ab2349, Abcam, USA) was used at twelfth day of endothelial differentiation to confirm the endothelial phenotype of differentiated cells. Before staining, the cells were fixed with 10% neutral buffered formalin for 20 min and washed with Dulbecco's Phosphate Buffered Saline (DPBS, PAA Laboratories GmbH, Austria).

Rabbit specific HRP/DAB detection kit (ab64261, Abcam, USA), was used for visualization according to the manufacturer's instruction. HRP/DAB detection kit included following components: Hydrogen Peroxide Block, Protein Block, Biotinylated goat anti-rabbit IgG, Streptavidin Peroxidase, DAB substrate and DAB chromogen. The cells were treated with Hydrogen Peroxide Block for 10 min, at room temperature (RT), and subsequently with Protein Block (5 min, RT) to avoid nonspecific background staining. After that, the cells were incubated with primary antibodies overnight, at 4 °C. Further, the cells were incubated with Biotinylated goat anti-rabbit IgG, and after that with Streptavidin Peroxidase and DAB chromogen mixed with DAB substrate. All incubations were performed for 10 min at RT. The cells were counterstained with Mayer's Hematoxylin for 1 min, rinsed, dehydrated, and covered with permanent mounting medium (VectaMount®, Vector laboratories, Burlingame, CA). Negative controls were cells treated by the same protocol but primary antibodies were excluded.

Experimental Animals

Adult, male, syngeneic BALB/c mice (Military Medical Academy, Belgrade, Serbia) were used. Each mouse was 22 ± 2 g weight, 8 weeks old, and kept in standard laboratory conditions. All the experiments on mice in this study were approved by the Local Ethical Committee (approval number 01-2857-8) and conducted in accordance with the Animal Welfare Act (Republic of Serbia).

Implantations

Bio-Oss®, size S, with granules 0.25–1 mm in size, PRP obtained from the blood of mice orbital sinus[22] and ADSCs at twelfth day of *in vitro* induced endothelial differentiation were used for the construction of implants.

Blood from mice orbital sinus was collected into the tubes which contained 4% sodium citrate as an anticoagulant, centrifugated, and the supernatant containing plasma with platelets was further processed. After the second centrifugation of supernatant from previous step, pellet with platelets was resuspended in small volume of supernatant plasma to get PRP. After counting in Malassez counting chamber (Paul Marienfeld GmbH & Co. KG, Lauda-Konigshofen, Germany), the established number of platelets was $1.89 \pm 0.5 \times 10^6$/mL. PRP was applied at concentration of 10% (v/v) in liquid component of the implant which was shown to be the optimal concentration for combining with ADSCs.[35,38]

The implants were prepared in sterile, flat glass plate. All implants were composed from 10 mg (~0.02 cm^3) of BC and 20 μL of liquid component. Two types of implants were made 1) **CP** type of implants constructed from 10 mg of **BC,** 18 μL of DMEM and 2 μL of **P**RP (finally 10% v/v), and 2) **ECP** type of implants constructed from 1×10^4 ADSCs differentiated into **E**Cs in 18 μL of DMEM and 2 μL of **P**RP (finally 10% v/v) as a liquid component, and 10 mg of **BC**. The cells were allowed to attach to the BC surface for 10–15 min before the implantations.[23] Each single implant was shaped in lump after clotting.[71]

Implantations were performed into the interscapular subcutaneous tissue of anesthetized mice. Large, sterile biopsy needle was used for the implantations. We had two experimental groups (ECP and CP) and four observation points (one, two, four and 8 weeks). Each group consisted of four animals per experimental period and totally sixteen implants per implantation period in one group.

Histology and Histomorphometry

Two and 8 weeks after implantation, the explants were fixed in 10% neutral buffered formalin, decalcified in 10% ethylenediaminetetraacetic acid (EDTA) solution (pH 7.4), dehydrated in ascending concen-

trations of ethanol, embedded in paraffin and sliced. The paraffin was removed with xylene, the sections were rehydrated in descending concentrations of ethanol. After that, Haematoxylin and Eosin (H&E) and Masson's Trichrome stainings were performed on 4 μm tissue sections from four different animals per group. Stained sections were analyzed by using light microscope LEICA DMR (Solms, Germany) and imaged by using LEICA DC 300 camera.

Histomorphometrical measurements were performed on total scans of H&E stained sections in the NIS-Elements software version 3.2 (Nikon, Tokyo, Japan). Total area of explants and total vessel area were measured by using "Annotations and Measurements" tool in the software. Percent of vascularization was calculated as: (total vessel area/total area of explants) * 100.

Immunohistochemistry

Prior to immunohistochemical analysis, the explants extracted after 2 and 8 weeks of implantation were processed as it was described for histological analysis. Primary antibodies anti-VEGFR-2 (1:200, ab 2349, Abcam, USA) and anti-osteocalcin (1:200, ab93876, Abcam, USA) were applied on 4 μm thick tissue sections. Before applying primary antibodies (4 °C, overnight), antigen-retrieval process was performed using 10 mM sodium citrate buffer (pH 6.0), in the microwave oven pre-warmed at 96 °C. For visualization, HRP/DAB detection kit was used according to the manufacturer's instruction (described in the section "Immunocytochemistry"). The tissue sections were counterstained with Mayer's Hematoxylin for 5 min, at RT, and mounted.

Quantitative Real-Time PCR

Whole RNA from the cells and implants was isolated using RNeasy Mini Kit® (Qiagen, Germany). Dnase I Rnase-free set (Qiagen, Germany) was applied for on-column digestion of residual DNA. RNA concentration in the samples was determined using Qubit® 2.0 fluorometer and Qubit® RNA assay kit (Invitrogen, Life technologies, USA).

Reverse transcription was performed with High-capacity cDNA Reverse Transcription Kit (Applied byosistems, Life Technologies, USA), in three steps (10 min at 25 °C; 120 min at 37 °C, and 5 min at 85 °C) in SureCycler 8800 (Agilent Technologies, USA).

Relative gene expression was assessed in Real-Time thermal cycler Stratagene MxPro-Mx3005P (Agilent Technologies, USA). Reactions were prepared using Kapa Sybr® Fast Universal 2× qPCR Master Mix (Kapa Biosystems, USA) and quantitect primer assays (Qiagen, Germany) for *von Willebrand factor* (*vWF*), vascular endothelial growth factor receptor 1 (*flt-1*), transcription factor early growth response-1 (*egr-1*), vascular cell adhesion molecule 1 (*vcam-1*) and osteopontin (*spp1*). A housekeeping gene for β-actin (*actb*) was used as a gene normalizator (Table 1). The results were expressed relative to the endothelial-related gene expression in the calibrator sample (untreated ADSCs, cultivated in DMEM until the third passage combined with PRP). Referent values of endothelial-related gene expression in the calibrator sample were denominated as "0".

Statistical Analysis

All statistical analyses were performed in the SPSS version 15.0 (SPSS Inc., Chicago, Illinois, USA). The mean values of relative gene expression levels and vascularization ± standard deviation were calculated, and Kruskal–Wallis non-parametric ANOVA test for the determination of statistical significance was applied. Statistically significant differences between tested groups at the same observation points were determined using *post hoc* Mann-Withney test. The differences were considered statistically significant for $p < 0.05$.

RESULTS

In Vitro Analysis

Twenty-four hours after the isolation, various cell types were seen (Fig. 1a). The cells from passage 0 (P0) to passage 3 (P3) became large, spindle-shaped and fibroblast-like (Fig. 1b), that is typical for mesenchymal cells. Numerous adherent, fibroblast-like, randomly oriented, and loosely adherent, round, epithelial-like cells at places were observed 7 days after P03 in standard cell culture media (Fig. 1c). Non-induced ADSCs formed populations of fibroblast-like cells 12 days after P03 (Fig. 1d). Monolayers of cells with cobblestone appearance were seen 7 days after inducing ADSCs into endothelial cells (Fig. 1e). On the twelfth day of endothelial differentiation, induced ADSC were connected *via* anastomoses built from cell membrane protrusions. They had the appearance of prevascular, capillary-like network (Fig. 1f).

At P03, ADSCs were $CD29^+$ (Fig. 2a) and $CD14^-$ (Fig. 2b). Twelve days after P03, non-induced ADSCs were fibroblast-like, and negative for VEGFR-2 (Fig. 2c). ADSCs induced towards endothelial cells were VEGFR-2 positive at the twelfth day of endothelial differentiation (Figs. 2d, 2e).

TABLE 1. List of primers used for qPCR.

Gene name	QuantiTect Primer assay	Detected transcript ID and length	Entrez gene ID
ACTB	Mm_Actb_2_SG, QT01136772	NM_007393 (1889 bp)	11,461
VWF	Mm_Vwf_1_SG, QT00116795	NM_011708 (8834 bp)	22,371
FLT-1	Mm_Flt1_1_SG, QT00096292	NM_010228 (6280 bp)	14,254
EGR-1	Mm_Egr1_1_SG, QT00265846	NM_007913 (3072 bp)	13,653
VCAM-1	Mm_Vcam1_1_SG, QT00128793	NM_011693 (3398 bp)	22,329
SPP1	Mm_Spp1_1_SG, QT00157724	NM_009263 (1428 bp)	20,750

Relative expression levels of endothelial-related genes in induced cells were checked at the third, seventh, twelfth, and fifteenth day of endothelial differentiation. The *vWF* and *flt-1* genes were the highest at the seventh day (Figs. 3a, 3b), while *egr-1* and *vcam-1* had the expression peak at the twelfth day of induced differentiation (Figs. 3c, 3d). Statistically significant increase in *vWF* expression during the endothelial differentiation was at 7-day in compare to a 3-day observation point, while *vWF* significantly decreased at 12-day in compare to a 7-day observation point (Fig. 3a). Increase in *flt-1* gene expression was statistically significant at 7-day comparing to a 3-day observation point (Fig. 3b). The *egr-1* gene statistically increased at 7-day comparing to a 3-day observation point and statistically decreased at 15-day in compare to a 12-day observation point (Fig. 3c), while *vcam-1* statistically decreased at 15-day-comparing to a 12-day observation point (Fig. 3d).

Histological and Histomorphometrical Analysis

At 2-week observation point, ECP implants had mild vascularization and a few multinucleated, osteoclast-like cells located around the particles of biomaterial (Fig. 4a). Connective tissue was mostly loose with weave-like collagen bundles (Fig. 5a), rich in fibroblast-like and polymorphonuclear cells (Fig. 4a) and in the places next to the BC particles collagen fibers were thick and well organized (Fig. 5a).

Mostly loose and regular connective tissue in places (Fig. 5d), weak cellularity and poor vascularization were seen in CP implants at 2-week observation point (Fig. 4d).

At 8-week observation point, ECP implants had large multinuclear cells and mild cellularization (Figs. 4b, 4c). Connective tissue was regular, with highly organized collagen fibers (Figs. 4b, 5b and 5c). Histologically, vascularization was greater than at previous observation point in the same type of implants and blood vessels were in the arrangement similar to branched and mature vascular network (Fig. 4c). Cuboidal-shaped, osteoblast-like cells were observed onto BC particles (Figs. 4b).

In CP group, at 8-week observation point, multinuclear cells adhered to the BC surface, while cellularity and vascularization were poorer than in EPC implants at the same observation point (Fig. 4e, 4f). Collagen fibers adjacent to the BC particles were thick but not well organized as in ECP implants at the same observation point. In the space more distant from the granules, the collagen fibers were weave-like (Fig. 5e, 5f).

The percentage of vascularization was higher in ECP than in CP group at 2-week observation point, but not statistically significant. A significantly higher percentage of vascularization was calculated for ECP compared with a CP group, at 8-week observation point (Fig. 6).

Immunohistochemical Analysis

In ECP implants, precursor-like cells were VEGFR-2^+ at both observation points (Figs. 7a, 7b). VEGFR-2 immunoexpression was weaker in CP group than in ECP group (Figs. 7e, 7f).

Osteocalcin (OC) immunoexpression was found in the space between biomaterial particles in ECP group, at both observation points (Figs. 7c, 7d), while in CP implants, OC immunoexpression was poor (Figs. 7g, 7h).

qPCR Analysis of Implants

At each observation point, *vWF* was significantly higher in CP than in the ECP group (Fig. 8a). In ECP group, the level of *flt-1* increased between 1- and 2-week observation point, and then slightly decreased at 8-week observation point (Fig. 8b). The *flt-1* was statistically higher in ECP than in the CP group at one-, two-, and 8-week observation point (Fig. 8b). In the CP implants, *flt-1* increased between one- and 4-week observation point, and decreased afterwards (Fig. 8b). In first two observation points (1- and 2-week), *egr-1* was down-regulated in both groups (Fig. 8c). In ECP implants, *egr-1* increased from the first to the last observation point which had statistical significance at 8-week observation point (Fig. 8c). The *egr-1* gene was

significantly higher in CP than in ECP group at 4-week observation point (Fig. 8c). In both groups, *vcam-1* was down-regulated at first two observation points, and up-regulated at 4-week observation point (Fig. 8d). At 8-week observation point, *vcam-1* was up-regulated in ECP implants, down-regulated in CP implants with statistical significance (Fig. 8d). *Spp1* was up-regulated in ECP and down-regulated in CP implants at each observation point, with statistical significance (Fig. 8e). In ECP implants, *spp1* was the highest at 2-week observation point, and later on slightly decreased (Fig. 8e).

DISCUSSION

Appropriate vascularization is essential for bone regeneration and in bone tissue bioengineering. To overcome inadequate development of blood vessels and consecutive failure of bone tissue regeneration, we examined the effect of ADSCs *in vitro* induced into ECs and combined with BC and PRP on vascularization and osteogenic process in subcutaneous implants. Ectopic osteogenesis model was chosen because it allows evaluation of *in vivo* angiogenic and osteogenic process, without the influence of factors from the bone.[50] Subcutaneous, interscapular implantations permit the evaluation of various features of the implanted biomaterial generally.[39] ECs can form vascular structures *in vitro* and anastomose with host vessels upon implantation.[60] Since low availability and proliferation capability limit the application of mature ECs[27] enriching the implants with mesenchymal stem cells (MSCs) induced into ECs can be a good alternative. Bone marrow-derived stem cells (BMSCs) were frequently used in BTE with promising results,[5,47] but low morbidity during tissue harvesting procedure[48] makes adipose tissue more optimal source of stem cells in compare to a bone marrow. Also, adipose tissue has much higher frequency of clonogenic mesenchymal progenitors than the bone marrow.[50]

For endothelial differentiation, $CD29^+/CD14^-$ ADSCs at P03 were used in our experiment. It was reported that the expression of CD29 increases in passaged cells compared to the cells from freshly isolated stromal vascular fraction (SVF).[58] Also, ADSCs are considered to be $CD14^-$,[7] and our ADSCs at P03 didn't express CD14. Likewise, we confirmed that the cells subjected to endothelial differentiation originated from adipose tissue, and not from circulating endothelial progenitors,[13] which has a monocyte/macrophage origin, and do express CD14.[46] $CD29^+/CD14^-$ ADSCs were induced into ECs, and expression dynamic of endothelial-related genes was assessed for 15 days.

Endothelial-related genes expression was the highest after seven or 12 days of differentiation. ADSCs started to express all examined genes except *vWF* from the third day of *in vitro* induced endothelial differentiation. The seventh day was shown to be crucial for *vWF* expression during *in vitro* endothelial differentiation. Konno and co-workers demonstrated that at seventh day of inducing ADSCs into ECs, ADSCs began to express *vWF*, which reached its highest level at tenth day of differentiation.[29] We have shown that *vWF* is up-regulated at seven-day observation point, and down-regulated at later observation points of *in vitro* differentiation. These differences could be explained by variations in conditions specific for each experiment.

Endothelial-cell phenotype was also confirmed by immunoexpression of VEGFR-2 at twelfth day of differentiation. ECs arise from the same precursors as the cells from hematopoietic lineage. The "switch" that controls differentiation of precursors to one of those lineages is VEGF, a mitogen typical for vascular ECs, which has two specific tyrosine kinase receptors—VEGFR-1/*flt-1*, and VEGFR-2/*flk-1*.[66] Our *in vitro* results regarding the expression of endothelial-related genes and VEGFR-2 immunoexpression were the selection criteria for choosing ADSCs at twelfth day of endothelial differentiation for implantations.

The impact of differentiated ADSCs on vascularization and osteogenic process was evaluated by comparing the groups with and without the cells. PRP was used in the control group because it contains highly concentrated platelets, which are critical in the wound healing process,[40] and our idea was to simulate natural bone repair. Inflammatory phase should be finished by week two during bone healing process, and bone repair is expected to be completed by 8 week, so we choose those two observation points for histological analysis.[51]

The hallmark features of a stable vascular network are morphological and functional heterogeneity of blood vessels.[2] In ECP implants, at 2-week observation point, these vessels had form and size conformed to the capillaries, arterioles and venules, while at 8-week observation point, vascularization was greater than at 2-week observation point, with dominant artery-like and vein-like blood vessels. Although CP implants were well-vascularized at 2-week observation point, vascular network wasn't developed at 8-week observation point. After the activation by an agonist such as calcium-chloride,[21] PRP releases various growth factors including VEGF, FGF, platelet-derived growth factor (PDGF), transforming growth factors (TGF-β_1 and TGF-β_2), interleukin-1 and platelet activating factor-4 which are considered to have an influence on increased vascularization and bone regeneration process.[1] However, the lifespan of these growth factors

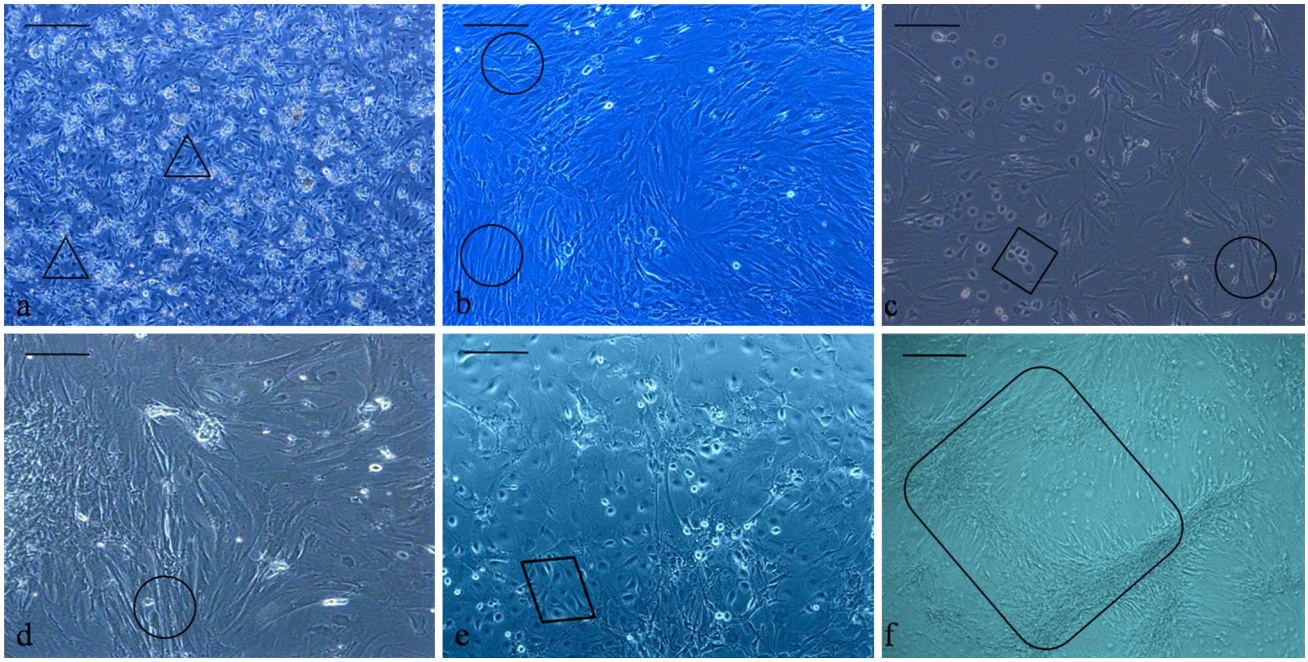

FIGURE 1. ***In vitro*** **analysis of ADSCs endothelial differentiation. (a) ADSCs 24 h after isolation; (b) ADSCs 1 day after P03 in DMEM; (c) ADSCs, DMEM, 7 days after P03; (d) ADSCs, DMEM, 12 days after P03 (e) ADSCs 7 days after induced endothelial differentiation; (f) ADSCs 12 days after induced endothelial differentiation. Magnification is 100×. Bar shows 100 μm. Legend: mesenchymal-like stem cells (triangle); fibroblast-like cells (circle), epithelial-like cells (rectangle), ''cobblestone'' cells (parallelogram), capillary-like structures (rounded rectangle).**

is short, limited to only 7–10 days,[12,36] which could be one of the explanations for unsustainability of the vascular network in CP implants. The results of our histomorphometric analysis showed that percentage of vascularization between groups, at both observation points was higher in ECP than in CP group, which was statistically significant at 8-week observation point. These results confirmed our histological observations which could be associated with the presence of ECs in ECP type of implants. So far, the beneficial effect of PRP mixed with ADSCs on vascularization was proved by combining PRP with either fresh[42] or expanded, non-differentiated ADSCs.[35] ADSCs induced *in vitro* towards ECs were used for implantations but only at orthotopic site[9] and with arteriovenous vascular bundle (AV-bundle).[65] Therefore, neither factors from the surrounding bone nor implanted blood vessels cannot be excluded. In an orthotopic critical-sized calvarial defect, rat ADSCs *in vitro* differentiated for 8 days into ECs and implanted, induced high microvessel density 8 weeks after the treatment, which was reflected on osteogenic process as a greater bone volume.[9] Rat ADSCs pre-differentiated into endothelial cells, incorporated in HAp-based scaffolds *in vitro* and implanted with AV-bundle caused significantly higher vessel density and vessel diameter than in the group with undifferentiated cells, HAp-based scaffold with AV-bundle and HAp-based scaffold only group.[65]

In our experiment, VEGFR-2 immunoexpression was seen in ECP implants at 2-week observation point, and slightly decreased at 8-week observation point, which is in accordance with the fact that VEGFR-2 is an early marker of angiogenesis.[20] VEGFR-2 is highly expressed in hemangioblasts, angioblasts, and endothelial cells.[25] We presumed that the abundance of VEGFR-2 positivity in ECP group is the result of *in vitro* endothelial differentiation of ADSCs which are the components of ECP implants. Implanted cells were positive for VEGFR-2 *in vitro*, which means that the cells were at various stages of endothelial differentiation at the time of implantation. Weaker VEGFR-2 immunoreactivity in CP implants might indicate that the combination of biomaterial carrier and PRP is suitable for the beginning, but insufficient for successful and sustainable vascularization.

In the implants, *vWf* expression was the highest at 4-week observation point in both groups, which is in accordance with its role in late angiogenesis.[54] During our observation, *vWF* expression increased at 1-week observation point in ECP implants, but stayed lower than in CP group and in the calibrator sample at each observation point. The reason for such expression

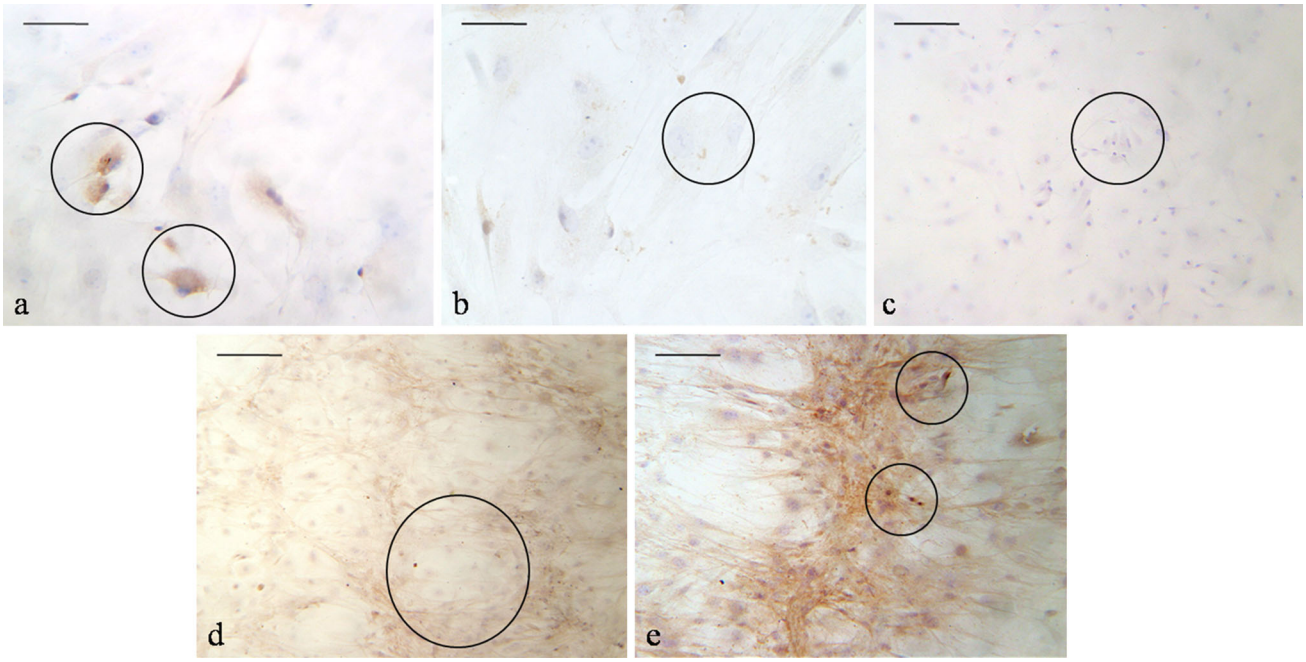

FIGURE 2. Immunocytochemical analysis of ADSCs endothelial differentiation. (a) ADSCs, P03, anti-CD29, magnification 200×, bar shows 50 μm, circled: CD29 positive cells; (b) ADSCs, P03, anti-CD14, magnification 200×, bar shows 50 μm, circled: CD14 negative cells; (c) non-induced ADSCs, day 12, magnification 100×, bar shows 100 μm, circled: VEGFR-2-negative cells; (d) ADSCs induced into ECs, day 12, anti-VEGFR-2, magnification 100×, bar shows 100 μm, circled: capillary-like structures containing lumen; (e) ADSCs induced into ECs, day 12, anti-VEGFR-2, magnification 200×, bar shows 50 μm, circled: VEGFR-2-positive cells.

pattern might be the fact that *vWF* was already expressed *in vitro*, and down-regulated at the time of implantation. *Flt-1* levels increased in ECP group at 2-week observation point, and slightly decreased later during the observation. *Flt-1* is expressed in angioblasts and ECs during the early embryonic development, and later declines.[14] Lower relative expression of *flt-1* in CP than in ECP implants could explain the unsustainability of vascular network in CP group at 8-week observation point. *Egr-1* regulates the expression of various genes, including *flt-1*.[17] In ECP implants, *egr-1* increased from 2- to 8-week observation point, while in CP ones *egr-1* had the expression peak at 4-week observation point. *Vcam-1* was down-regulated at first two observation points, in both groups. ECs are constantly exposed to pulsatile blood flow, a generator of specific mechanical force-wall shear stress, which changes their morphology and functions in various ways including down-regulation of *vcam1*,[30] which could explain the results we have obtained at earlier observation points. At 4-week observation point, *vcam-1* was up-regulated in both groups that might be related to the presence of polymorphonuclears observed histologically at 2-week observation point. Particularly, VCAM-1 mediates leukocyte binding to the ECs *via* interaction with its integrin counterreceptor-very late activation antigen-4 (VLA-4) on leucocytes.[11]

Histological analysis of bone matrix deposition conducted on Masson's Trichrome stained tissue sections revealed mostly loose, and regular connective tissue in places at 2-week observation point in both type of implants. Thin collagen fibers were seen in both types of implants at 8-week observation point, but despite of it collagen fibers adjacent to the BC particles in CP implants were not well organized as in ECP type of implants at the same observation point. Also, higher degree of presence of osteoblast-like cells was seen in ECP than in CP implants at 8-week observation point. The explanation for such histological picture in the implants with ADSCs induced into ECs might be the fact that ECs release growth factors such as bone morphogenic protein-2, endothelin-1, and insulin-like growth factor, with the influence on the differentiation of osteogenic precursors.[9] Osteoblasts release VEGF, which acts on ECs and promotes angiogenesis.[49] It could be presumed that the differentiation of precursors in ECP implants to osteoblasts was regulated by ECs, so we hypothesized that such interaction occurred among those cell types in ECP group. In addition to that, ECP implants had stronger immunoexpression of bone specific protein osteocalcin onto biomaterial particles and between them at both observation points, which can be associated with the activity of osteoblast-like cells. Weaker osteocalcin immunoexpression at

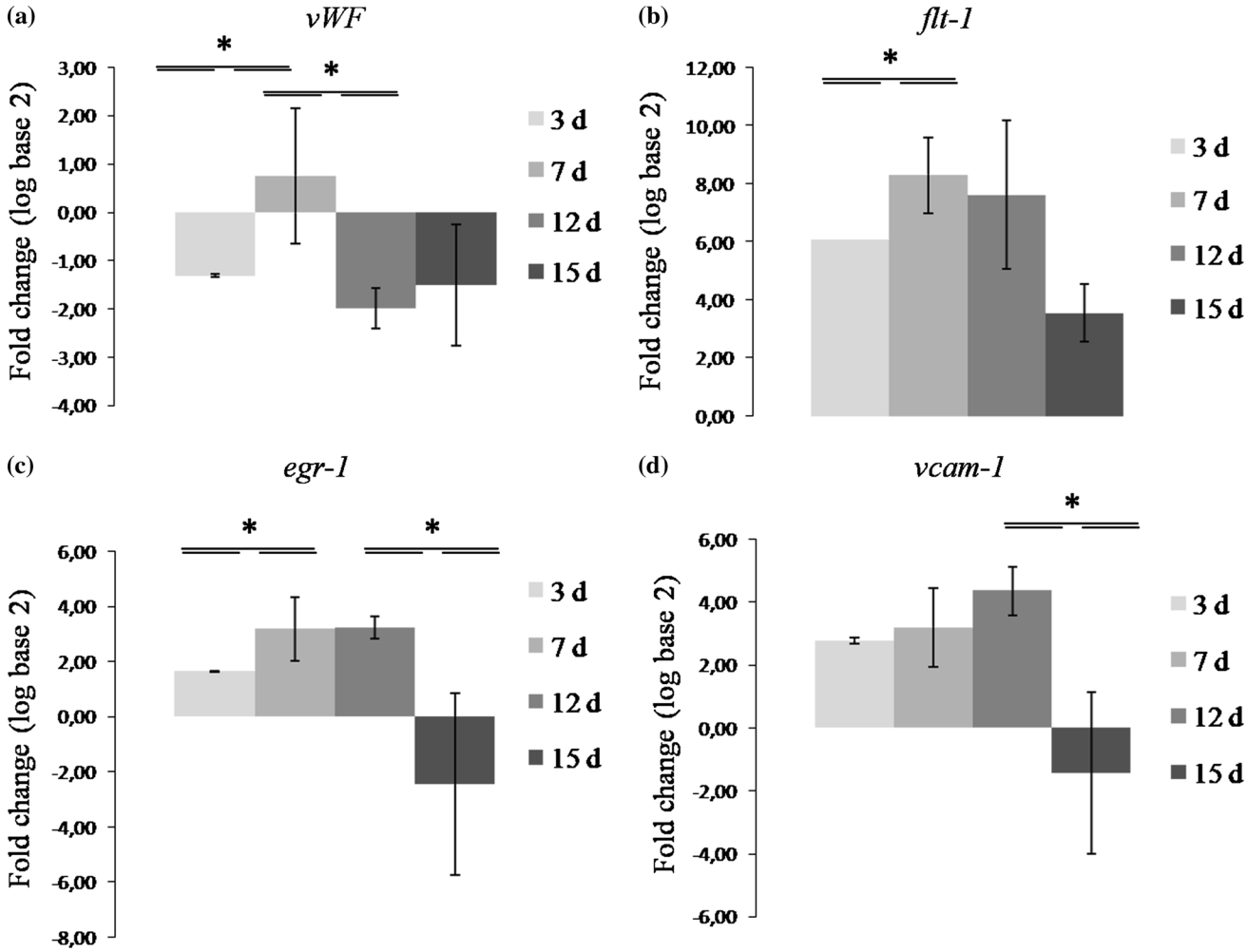

FIGURE 3. Fold changes (log base 2) of selected genes, at third, seventh, twelfth, and fifteenth day (day = d) of induced endothelial differentiation relative to the calibrator sample. (a) Relative expression of *vWF*, (b) Relative expression of *flt-1*, (c) Relative expression of *egr-1*, (d) Relative expression of *vcam-1*. Legend: *Statistical significance ($p < 0.05$) between gene-expression levels at 3, 7, 12 and 15 days of endothelial differentiation.

2-week observation point than at 8-week observation point in both types of implants is expected because osteocalcin is a late marker of bone formation.[31] Unlike osteocalcin, osteopontin is not bone specific, but it has an important role in bone remodeling process.[19] The regulation of osteopontin gene, *spp1*, is reciprocally coordinated by osteoblasts and osteoclasts, in a way that *spp1* expression in osteoblasts is inhibited at bone formation sites when the expression in osteoclasts at resorption sites is stimulated.[18] It could be presumed that *spp1* was up-regulated in the group of implants enriched with ADSCs induced into ECs, at each observation point, because osteoblast-like and multinucleated cells were abundant. Poor cellularity in CP group might be the reason for down-regulation of *spp-1*.

Literature data about the impact of bone mineral matrix combined with PRP on osteogenic process indicate mainly on favorable effects. Kim and his co-workers have shown that bone density in rabbit cranial defects filled with Bio-Oss® + Plasma Rich in Growth Factors (PRGF) was higher than in the group with Bio-Oss® only.[26] Also, bone formation in rabbit cranial defects increased in the presence of bone mineral matrix Bio-Oss® combined with PRP,[1,52] than when only Bio-Oss® was implanted. On the other side, You *et al.* used PRP as an adjunct to Bio-Oss® in treating bone defects around titanium dental implants in mongrel dogs and gained significantly lower percentage of bone-implant contact in the defects treated with Bio-Oss® plus PRP than in the defects with PRP only.[67]

CONCLUSION

ADSCs *in vitro* induced towards ECs in combination with PRP and bone mineral matrix increased

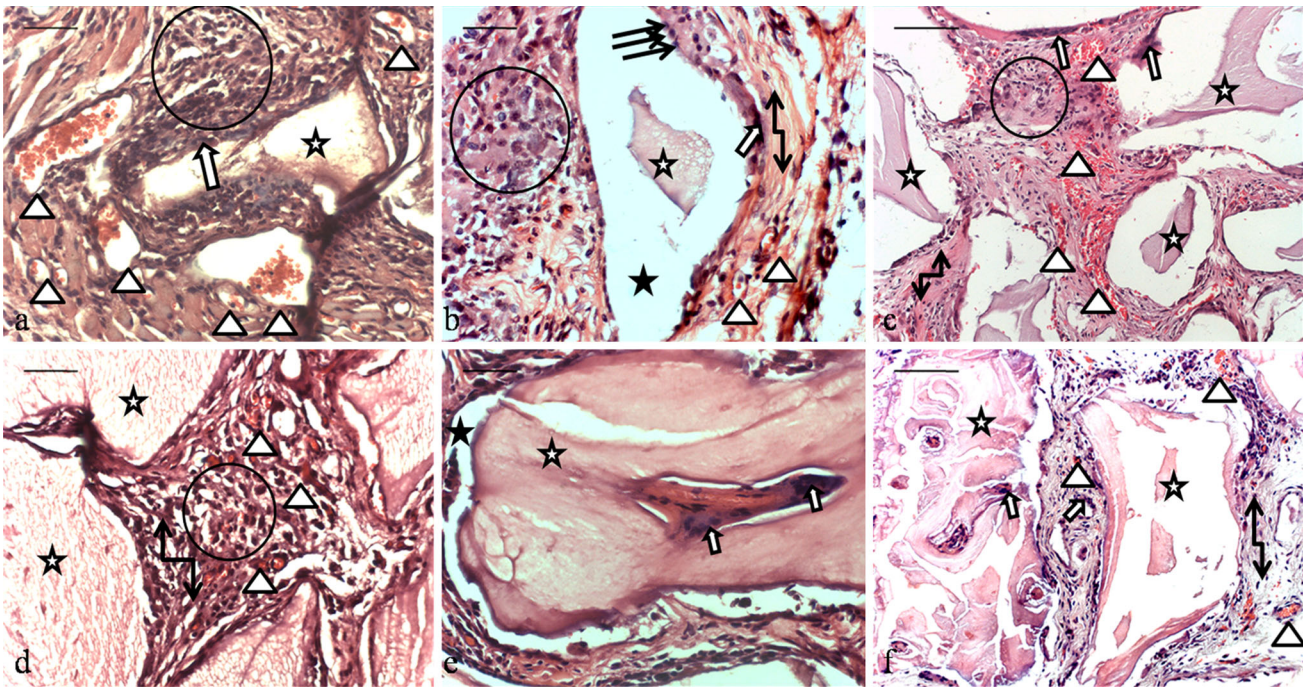

FIGURE 4. H&E stained implants and histomorphometry. (a) ECP implants, week 2, magnification 400×, bar shows 20 μm; (b) ECP implants, week 8, magnification 400×, bar shows 20 μm; (c) ECP implants, week 8, magnification 200×, bar shows 50 μm; (d) CP implants, week 2, magnification 400×, bar shows 20 μm; (e) CP implants, week 8, magnification 400×, bar shows 20 μm; (f) CP implants, week 8, magnification 200×, bar shows 50 μm. Legend: multinuclear cell (thick white arrow), collagen (black rectangular arrow), osteoblast-like cells (thin black arrow), blood vessels (arrowheads), biomaterial particles (white star), cellularization (circle).

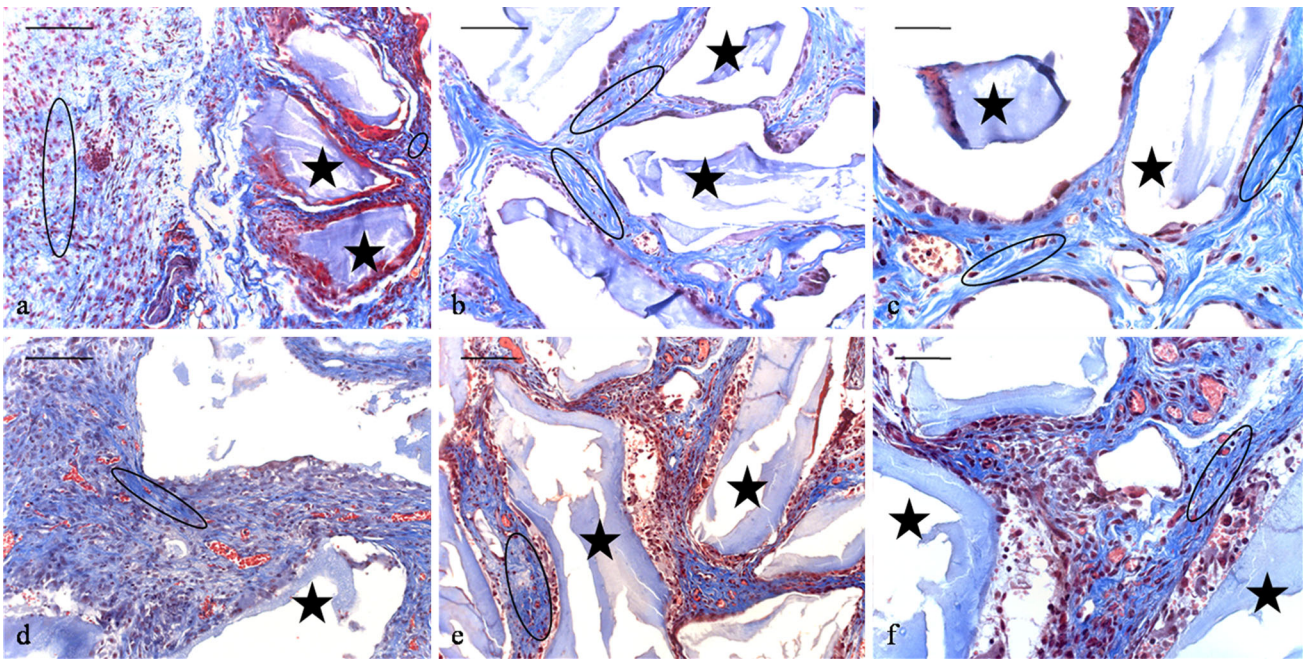

FIGURE 5. Masson's Trichrome stained implants. (a) ECP implants, week 2, magnification 200×, bar shows 50 μm; (b) ECP implants, week 8 magnification 200×, bar shows 50 μm; (c) ECP implants, week 8, magnification 400×, bar shows 20 μm; (d) CP implants, week 2, magnification 200×, bar shows 50 μm; (e) CP implants, week 8, magnification 200×, bar shows 50 μm; (f) CP implants, week 8, magnification 400×, bar shows 20 μm Legend: collagen (ellipse), biomaterial particles (black star).

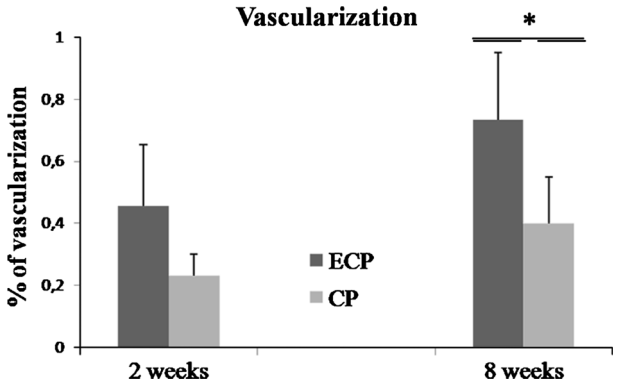

FIGURE 6. Percentage of vascularization in ECP and CP implants at 2 and 8 weeks. *Significant differences between groups, within the same observation point for $p < 0.05$.

vascularization in bioengineered implants subcutaneously implanted, which was confirmed by endothelial-related gene expression, high percentage of vascularization and VEGFR-2 immunoexpression. Immunoexpression of osteocalcin, relative expression of *spp1* and histological analysis showed that osteogenic process was more pronounced when the carrier was loaded with ADSCs induced into ECs, which can be associated with the strong vascularization in cellularized implants. In implants without the cells vasculogenesis was initially stimulated, but vascular network was unsustainable at later observation points. Therefore, the approach that includes ADSCs *in vitro* induced into ECs combined with BC and PRP can be a good strategy for improving vascularization

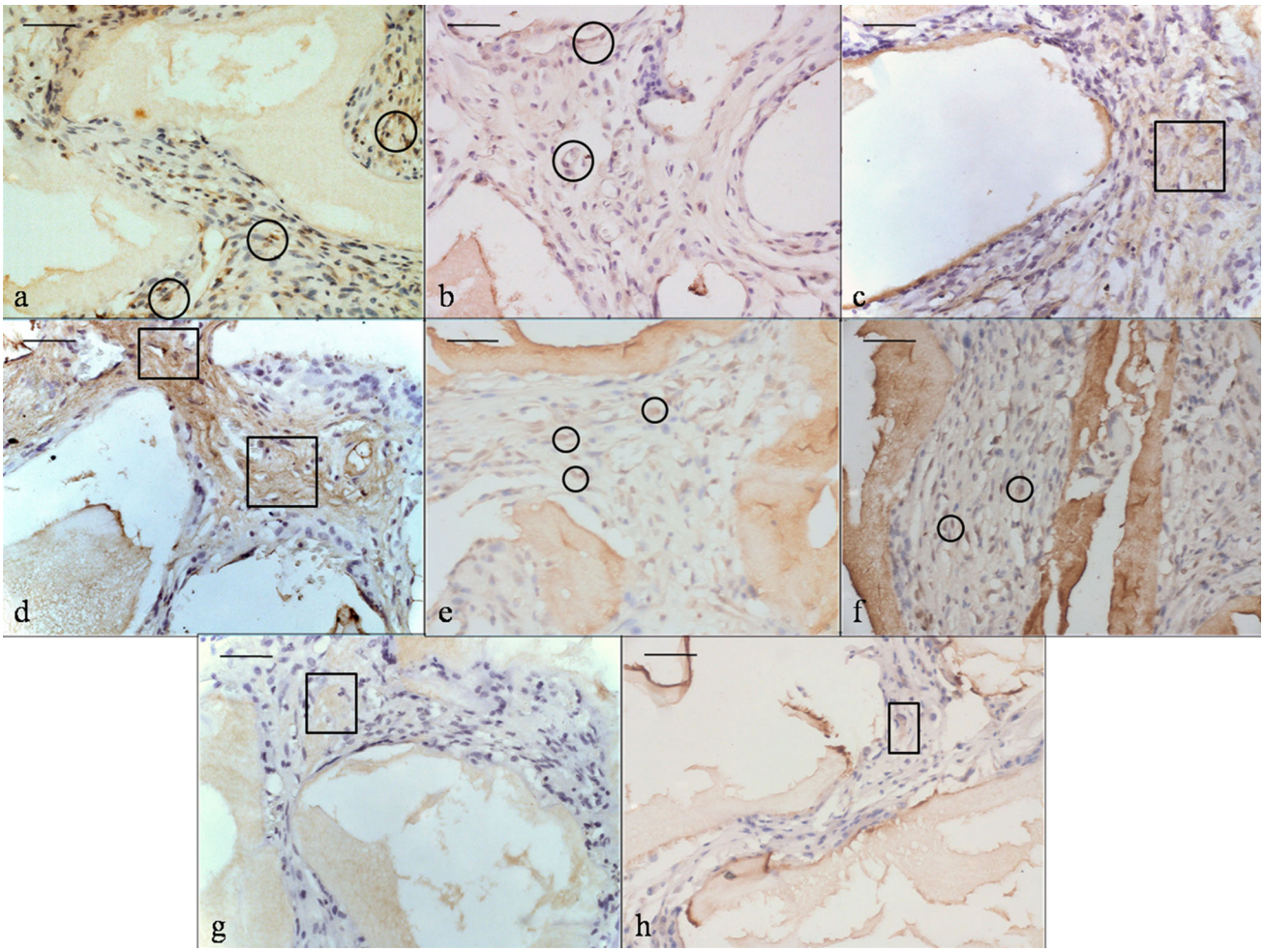

FIGURE 7. Immunohistochemical analysis of the implants. (a) ECP implants, week 2, anti-VEGFR-2; (b) ECP implants, week 8, anti-VEGFR-2, (c) ECP implants, week 2, anti-OC; (d) ECP implants, week 8; (e) CP implants, week 2, anti-VEGFR-2; (f) CP implants, week 8, anti-VEGFR-2; (g) CP implants, week 2, anti-OC; (h) CP implants, week 8, anti-OC. Magnification is 400×. Bar shows 20 μm; Legend: VEGFR-2 immunoexpression (circle), OC immunoexpression (rectangular).

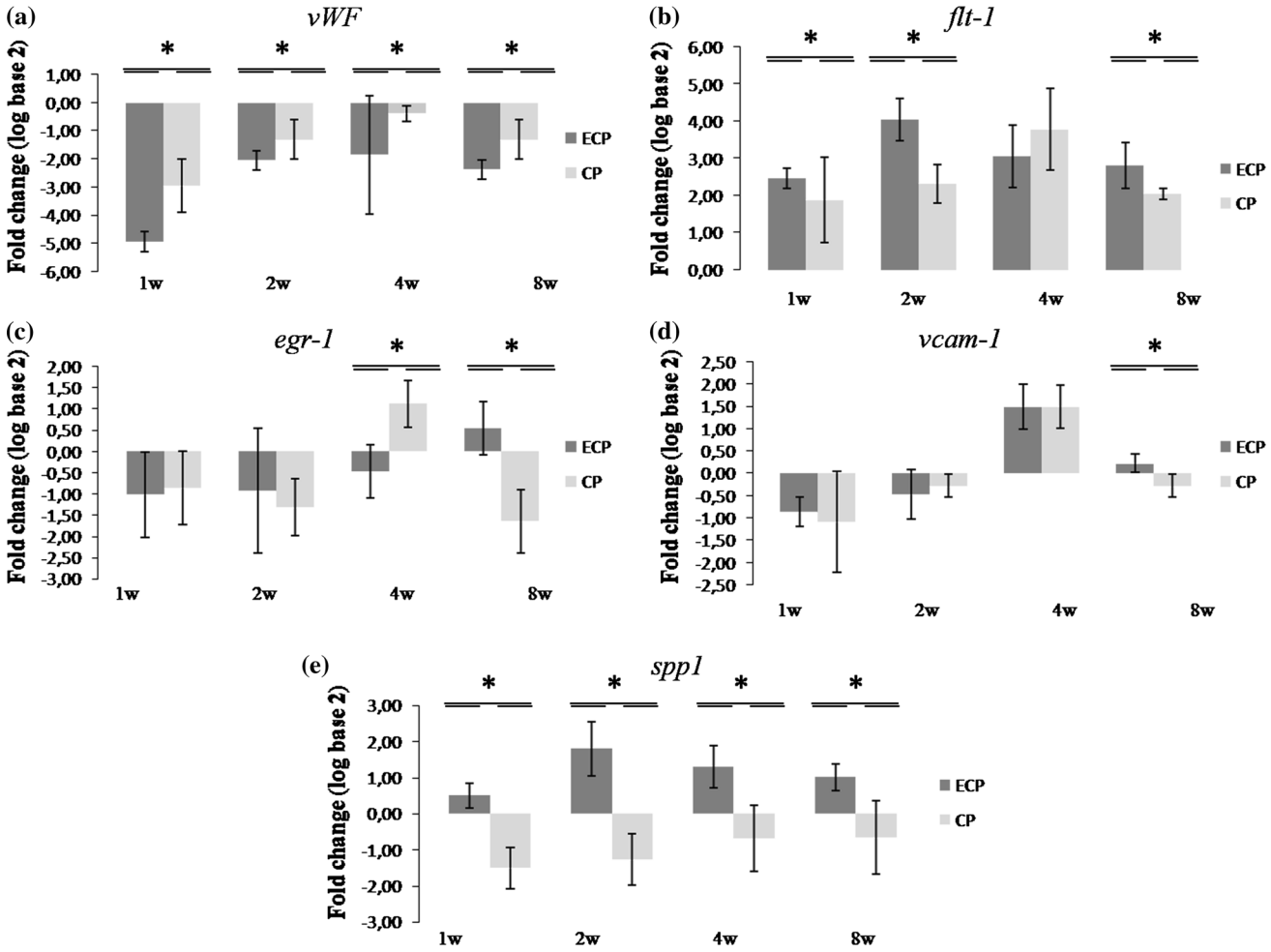

FIGURE 8. Fold changes (log base 2) of selected genes relative to the calibrator sample in ECP and CP implants. (a) Relative expression of *vWF*, (b) relative expression of *flt-1*, (c) relative expression of *egr-1*, (d) relative expression of *vcam-1*, (e) relative expression of *spp1*. Legend: w—week. * Statistical significance ($p < 0.05$) between groups within the same observation point.

in BTE. Also, obtained data about the impact of ECs in cellularized implants on vascularization and osteogenic process represent the main benefit of our study which can be further integrated with some of the described strategies for improving vascularization in BTE.

ACKNOWLEDGMENTS

This work was supported by Project Grant III41017, Ministry of Education, Science and Technological Development, Republic of Serbia. The authors would like to thank Tanja Prokić, a technician from Faculty of Medicine, University of Niš, for helping with animal procedures and tissue processing.

CONFLICT OF INTEREST

Jelena G Najdanović, Vladimir J Cvetković, Sanja Stojanović, Marija Đ Vukelić-Nikolić, Milica N Stanisavljević, Jelena M Živković and Stevo J Najman declare that they have no conflicts of interest.

ETHICAL STANDARDS

No human studies were carried out by the authors for this article. All animal procedures were approved by the Local Ethical Committee (approval number 01-2857-8) and conducted in accordance with the Animal Welfare Act (Republic of Serbia). The animals were treated conforming to the regulation of the "European Convention for the Protection of Vertebrate Animals used for Experimental and Other Scientific Purposes (ETS no. 123 Appendix A)".

REFERENCES

[1]Aghaloo, T. L., P. K. Moy, and E. G. Freymiller. Evaluation of platelet rich plasma in combination with freeze-dried bone in the rabbit cranium. A pilot study. *Clin. Oral Implants Res*. 16:250–257, 2005.

[2]Aitsebaomo, J., A. L. Portbury, J. C. Schisler, and C. Patterson. Brothers and sisters: molecular insights into arterial-venous heterogeneity. *Circ. Res*. 103:929–939, 2008.

[3]Ajduković, Z., S. Najman, Lj. Đorđević *et al*. Repair of bone tissue affected by osteoporosis with hydroxyapatite-poly-L-lactide (HAp-PLLA) with and without blood plasma. *J. Biomater. Appl*. 20:179–190, 2005.

[4]Anderson, S. M., S. N. Siegman, and T. Segura. The effect of vascular endothelial growth factor (VEGF) presentation within fibrin matrices on endothelial cell branching. *Biomaterials* 32:7432–7443, 2011.

[5]Arinzeh, T. L. S. J. Peter, M. P. Archambault *et al*. Allogeneic mesenchymal stem cells regenerate bone in a critical-sized canine segmental defect. *J. Bone Joint Surg (Am.)* 85:1927–1935, 2003.

[6]Azuma, N., S. A. Duzgun, M. Ikeda, *et al*. Endothelial cell response to different mechanical forces. *J. Vasc. Surg*. 32:789, 2000.

[7]Cai, X., X. Su, G. Li, *et al*. Osteogenesis of adipose-derived stem cells, osteogenesis, edited by Y. Lin (Ed.), 2012 http://www.intechopen.com/books/osteogenesis/osteogenesis-of-adipose-derived-stem-cells.

[8]Conrad, C., and R. Huss. Adult stem cell lines in regenerative medicine and reconstructive surgery. *J. Surg. Res*. 124(2):201–208, 2005.

[9]Cornejo, A., D. E. Sahar, S. M. Stephenson, *et al*. Effect of adipose tissue-derived osteogenic and endothelial cells on bone allograft osteogenesis and vascularization in critical-sized calvarial defects. *Tissue Eng. Part A* 18:15–16, 2012.

[10]Druecke, D., S. Langer, E. Lamme, *et al*. Neovascularization of poly(ether ester) blockcopolymer scaffolds in vivo: long-term investigations using intravital fluorescent microscopy. *J. Biomed. Mater. Res. A* 68A:10–18, 2004.

[11]Elices, M. J., L. Osborn, Y. Takada, *et al*. VCAM- I on activated endothelium interacts with the leukocyte integrin VLA-4 at a site distinct from the VLA-4/fibronectin binding site. *Cell* 60:577–584, 1990.

[12]Eppley, B. L., W. S. Pietrzak, M. Blanton, *et al*. Platelet-rich plasma: a review of biology and applications in plastic surgery. *Plast. Reconstr. Surg*. 118:147e–159e, 2006.

[13]Fernandez Pujol B., F. C. Lucibello, U. M. Gehling, *et al*. Endothelial-like cells derived from human CD14 positive monocytes. Differentiation 65:287–300, 2000.

[14]Fong, G. H., J. Rossant, M. Gertsenstein, and M. L. Breitman. Role of the Flt-1 receptor tyrosine kinase in regulating the assembly of vascular endothelium. *Nature* 376:66–70, 1995.

[15]Fraser, J. K., I. Wulur, Z. Alfonso, and M. H. Hedrick. Fat tissue: an underappreciated source of stem cells for biotechnology. *Trends Biotechnol*. 24:150–154, 2006.

[16]Freshney, R. I. Culture of Animal Cells—A Manual of Basic Technique (5th ed.). New York: Wiley, pp. 192–195, 2005.

[17]Gashler, A., and V. P. Sukhatme. Early growth response protein 1 (Egr-1): prototype of a zinc finger family of transcription factors. *Prog. Nucleic Acid Res. Mol. Biol*. 50:191–224, 1995.

[18]Gluhak-Heinrich, J., A. Villarreal, and D. Pavlin. Reciprocal regulation of osteopontin gene during mechanically induced bone formation and resorption. *J. Bone Miner. Res*. 15:S1, S478, 2000.

[19]Gürsoy, G., Y. Acar, and S. Alagöz. Osteopontin: A multifunctional molecule. *J. Med. Med. Sci*. 1:055–060, 2010.

[20]Hoeben, A., B. Landuyt, and M. S. Highley. Vascular endothelial growth factor and angiogenesis. *Pharmacol. Rev*. 56:549–580, 2004.

[21]Intini, G. The use of platelet-rich plasma in bone reconstruction therapy. *Biomaterials* 30:4956–4966, 2009.

[22]Intini, G., S. Andreana, F. E. Intini, *et al*. Calcium sulfate and platelet-rich plasma make a novel osteoinductive biomaterial for bone regeneration. *J. Transl. Med*. 5:13, 2007.

[23]Jurgens, W. J., R. J. Kroeze, R. A. Bank, *et al*. Rapid attachment of adipose stromal cells on resorbable polymeric scaffolds facilitates the one-step surgical procedure for cartilage and bone tissue engineering purposes. *J. Orthop. Res*. 29:853–860, 2011.

[24]Kanczler, J. M., and R. O. Oreffo. Osteogenesis and angiogenesis: the potential for engineering bone. *Eur. Cell. Mater*. 215:100–114, 2008.

[25]Karamysheva, A. F. Mechanisms of angiogenesis. *Biochemistry (Moscow)* 73:751–762, 2008.

[26]Kim, E. S., E. J. Park, and P. H. Choung. Platelet concentration and its effect on bone formation in calvarial defects: an experimental study in rabbits. *J. Prosthet. Dent*. 86:428–433, 2001.

[27]Kim, S., and H. Von Recum. Endothelial stem cells and precursors for tissue engineering: cell source, differentiation, selection, and application. *Tissue Eng. B* 14:133–147, 2008.

[28]Ko, H. C., B. K. Milthorpe, and C. D. McFarland. Engineering thick tissues—the vascularisation problem. *Eur. Cells Mater*. 14:1–18, 2007.

[29]Konno, M., T. S. Hamazaki, S. Fukuda, *et al*. Efficiently differentiating vascular endothelial cells from adipose tissue-derived mesenchymal stem cells in serum-free culture. *Biochem. Biophys. Res. Commun*. 400:461–465, 2010.

[30]Korenaga, R., J. Ando, K. Kosaki, *et al*. Negative transcriptional regulation of the VCAM-1 gene by fluid shear stress in murine endothelial cells. *Am. J. Physiol*. 273:C1506–C1515, 1997.

[31]Lee, A. J., S. Hodges, and R. Eastell. Measurement of osteocalcin. *Ann. Clin. Biochem*. 37:432–446, 2000.

[32]Lin, C. S., Z. C. Xin, C. H. Deng, *et al*. Defining adipose tissue-derived stem cells in tissue and in culture. *Histol. Histopathol*. 25:807–815, 2010.

[33]Lysiak-Drwal, K., M. Dominiak, L. Solski, *et al*. Early histological evaluation of bone defect healing with and without guided bone regeneration techniques: experimental animal studies. *Postepy Hig Med Dosw (Online)* 62:282–288, 2008.

[34]Madonna, R., and R. De Caterina. *In vitro* neovasculogenic potential of resident adipose tissue precursors. *Am. J. Physiol. Cell Physiol*. 295:C1271–C1280, 2008.

[35]Man, Y., P. Wang, Y. Guo, *et al*. Angiogenic and osteogenic potential of platelet-rich plasma and adipose-derived stem cell laden alginate microspheres. *Biomaterials* 33:8802–8811, 2012.

[36]Marx, R. E., E. R. Carlson, R. M. Eichstaedt, *et al*. Platelet-rich plasma: growth factor enhancement for bone grafts. *Oral Surg. Oral Med. Oral Pathol. Oral Radiol. Endod*. 85:638–646, 1998.

[37]Mizuno, H. Adipose-derived stem cells for tissue repair and regeneration: ten years of research and literature review. *J. Nippon Med. Sch.* 76:56–66, 2009.
[38]Murphy, M. B., D. Blashki, R. M. Buchana, *et al.* Multicomposite bioactive osteogenic sponges featuring mesenchymal stem cells, platelet-rich plasma, nanoporous silicon enclosures, and peptide amphiphiles for rapid bone regeneration. *J. Funct. Biomater.* 2:39–66, 2011.
[39]Najman, S., Lj. Đorđević, V. Savić, *et al.* Changes of HAp/PLLA biocomposites and tissue reaction after subcutaneous implantation. *Facta Univ. Ser. Med. Biol.* 10:131–134, 2003.
[40]Nurden, A. T., P. Nurden, M. Sanchez, *et al.* Platelets and wound healing. *Front Biosci.* 13:3525–3548, 2008.
[41]Ochoa, E. R., and J. P. Vacanti. An overview of the pathology and approaches to tissue engineering. *Ann. N.Y. Acad. Sci.* 979:10–26, 2002.
[42]Pak, J., J. J. Chang, J. H. Lee, and S. H. Lee. Safety reporting on implantation of autologous adipose tissue-derived stem cells with platelet-rich plasma into human articular joints. *BMC Musculoskelet. Disord.* 14:337, 2013.
[43]Partap, S., F. Lyons, and F. J. O'Brien. Scaffolds & Surfaces. *Stud. Health Technol. Inform.* 152:187–201, 2010.
[44]Patel, Z. S., S. Young, Y. Tabata, *et al.* Dual delivery of an angiogenic and an osteogenic growth factor for bone regeneration in a critical size defect model. *Bone* 43:931, 2008.
[45]Piattelli, M., G. A. Favero, A. Scarano, *et al.* Bone reactions to anorganic bovine bone (Bio-Oss) used in sinus augmentation procedures: a histologic long-term report of 20 cases in humans. *Int. J. Oral Maxillofac. Implants* 14:835–840, 1999.
[46]Planat-Benard, V., J. S. Silvestre, B. Cousin, *et al.* Plasticity of human adipose lineage cells toward endothelial cells: physiological and therapeutic perspectives. *Circulation* 109:656, 2004.
[47]Quarto, R., M. Mastrogiacomo, R. Cancedda, *et al.* Repair of large bone defects with the use of autologous bone marrow stromal cells. *N. Engl. J. Med.* 344:385–386, 2001.
[48]Sandor, G. K., and R. Suuronen. Combining adipose-derived stem cells, resorbable scaffolds and growth factors: an overview of tissue engineering. *J. Can. Dent. Assoc.* 74:167–170, 2008.
[49]Santos, M. I., and R. L. Reis. Vascularization in bone tissue engineering: physiology, current strategies, major hurdles and future challenges. *Macromol. Biosci.* 10:12–27, 2010.
[50]Scherberich, A., A. M. Müller, D. J. Schäfer, *et al.* Adipose tissue-derived progenitors for engineering osteogenic and vasculogenic grafts. *J. Cell. Physiol.* 225:348–353, 2010.
[51]Shapiro, F. Bone development and its relation to fracture repair, The role of mesenchymal osteoblasts and surface osteoblasts. *Eur. Cell. Mater.* 15:53–76, 2008.
[52]Shayesteh, Y. S., A. Khorsand, P. Motahhary, *et al.* Evaluation of platelet-rich plasma in combination with deproteinized bovine bone mineral in the rabbit cranium; pilot study. *J. Dent.* 2:127–134, 2005.
[53]Soker, S., M. Machado, and A. Atala. Systems for therapeutic angiogenesis in tissue engineering. *World J. Urol.* 18:10–18, 2000.
[54]Starke, R. D., F. Ferraro, K. E. Paschalaki, *et al.* Endothelial von Willebrand factor regulates angiogenesis. *Blood* 117:1071–1080, 2011.
[55]Sun, H., Z. Qu, Y. Guo, *et al. In vitro* and in vivo effects of rat kidney vascular endothelial cells on osteogenesis of rat bone marrow mesenchymal stem cells growing on polylactide-glycoli acid (PLGA) scaffolds. *Biomed. Eng. Online* 6:41, 2007.
[56]Sun, G., Y. I. Shen, S. Kusuma, *et al.* Functional neovascularization of biodegradable dextran hydrogels with multiple angiogenic growth factors. *Biomaterials* 32:95–106, 2011.
[57]Sung, J. H., H. M. Yang, J. B. Park, *et al.* Isolation and characterization of mouse mesenchymal stem cells. *Transpl. Proc.* 40:2649–2654, 2008.
[58]Traktuev, D. O., E. V. Parfenova, V. A. Tkachuk, K. L. March, *et al.* Adipose stromal cells-plastic type of cells with high therapeutic potential. *Tsitologiia* 48:83–94, 2006.
[59]Traktuev, D. O., D. N. Prater, S. Merfeld-Clauss, *et al.* Robust functional vascular network formation in vivo by cooperation of adipose progenitor and endothelial cells. *Circ. Res.* 104:1410–1420, 2009.
[60]Tremblay, P. L., V. Hudon, F. Berthod, *et al.* Inosculation of tissue-engineered capillaries with the host's vasculature in a reconstructed skin transplanted on mice. *Am. J. Transpl.* 5:1002–1010, 2005.
[61]Unger, R. E., A. Sartoris, K. Peters, *et al.* Tissue-like self-assembly in cocultures of endothelial cells and osteoblasts and the formation of microcapillary-like structures on three-dimensional porous biomaterials. *Biomaterials* 28:3965, 2007.
[62]Von Offenberg Sweeney, N., P. M. Cummins, E. J. Cotter, *et al.* Cyclic strain-mediated regulation of vascular endothelial cell migration and tube formation. *Biochem. Biophys. Res. Commun.* 329:573–582, 2005.
[63]Wang, D. S., M. Miura, H. Demura, and K. Sato. Anabolic effects of 1,25-dihydroxyvitamin D3 on osteoblasts are enhanced by vascular endothelial growth factor produced by osteoblasts and by growth factors produced by endothelial cells. *Endocrinology* 138:2953–2962, 1997.
[64]Xie, X., Y. Wang, C. Zhao, *et al.* Comparative evaluation of MSCs from bone marrow and adipose tissue seeded in PRP-derived scaffold for cartilage regeneration. *Biomaterials* 33:7008–7018, 2012.
[65]Yang, P., X. Huang, J. Shen, *et al.* Development of a new pre-vascularized tissue-engineered construct using pre-differentiated rADSCs, arteriovenous vascular bundle and porous nano-hydroxyapatide-polyamide 66 scaffold. *BMC Musculoskelet. Disord.* 14:318, 2013.
[66]Yang, Y. Q., T. Ying-Ying, and W. Ricky. The role of vascular endothelial growth factor in ossification. *Int. J. Oral Sci.* 4:64–68, 2012.
[67]You, T. M., B. H. Choi, J. Li, *et al.* The effect of platelet-rich plasma on bone healing around implants placed in bone defects treated with Bio-Oss: a pilot study in the dog tibia. *Oral Surg. Oral Med. Oral Pathol. Oral Radiol. Endod.* 103:e8–e12, 2007.
[68]Young, S., J. D. Kretlow, C. Nguyen, *et al.* Microcomputed tomography characterization of neovascularization in bone tissue engineering applications. *Tissue Eng. Part B Rev.* 14:295–306, 2008.
[69]Yu, H., P. J. VandeVord, L. Mao, *et al.* Improved tissue-engineered bone regeneration by endothelial cell mediated vascularization. *Biomaterials* 30:508–517, 2009.
[70]Zhang, N., Y. P. Wu, S. J. Qian *et al.* Research progress in the mechanism of effect of PRP in bone deficiency healing. *Sci. World J.* 1–7. ID 134582, 2013.
[71]Živkovic, J. M., S. J. Najman, M. Đ. Vukelić *et al.* Osteogenic effect of inflammatory macrophages loaded onto mineral bone substitute in subcutaneous implants. *Arch. Biol. Sci.* 67(1):173–186, 2015.